Check for updates

NIST Internal Report
NIST IR 8563

Industrial Wireless non-Communications Aggressor Reproduction

A Playback Approach for TIG Welding Measurements

Mohamed Kashef (Hany)
Jing Geng
Richard Candell

This publication is available free of charge from:
https://doi.org/10.6028/NIST.IR.8563

NATIONAL INSTITUTE OF STANDARDS AND TECHNOLOGY
U.S. DEPARTMENT OF COMMERCE

NIST Internal Report
NIST IR 8563

Industrial Wireless non-Communications Aggressor Reproduction

A Playback Approach for TIG Welding Measurements

Mohamed Kashef (Hany)
Jing Geng
Richard Candell
Smart Connected Systems Division
Communications Technology Laboratory

This publication is available free of charge from:
https://doi.org/10.6028/NIST.IR.8563

February 2025

U.S. Department of Commerce
Jeremy Pelter, Acting Secretary of Commerce

National Institute of Standards and Technology
Craig Burkhardt, Acting Under Secretary of Commerce for Standards and Technology and Acting NIST Director

Certain equipment, instruments, software, or materials, commercial or non-commercial, are identified in this paper in order to specify the experimental procedure adequately. Such identification does not imply recommendation or endorsement of any product or service by NIST, nor does it imply that the materials or equipment identified are necessarily the best available for the purpose.

NIST Technical Series Policies
Copyright, Use, and Licensing Statements
NIST Technical Series Publication Identifier Syntax

Publication History
Approved by the NIST Editorial Review Board on 2025-02-07

How to cite this NIST Technical Series Publication:
Mohamed Kashef (Hany), Jing Geng, Richard Candell (2025) Industrial Wireless non-Communications Aggressor Reproduction: A Playback Approach for TIG Welding Measurements. (National Institute of Standards and Technology, Gaithersburg, MD), NIST IR 8563. https://doi.org/10.6028/NIST.IR.8563

Author ORCID iDs
Mohamed Kashef (Hany): 0000-0002-6619-3509
Jing Geng: 0000-0001-9256-2075
Richard Candell: 0000-0002-6679-8823

Abstract

Industrial Wireless system performance can be degraded by various factors (aggressors) found in operational environments. Non-communications electromagnetic aggressors are defined as any over-the-air emissions that lower communications performance of the industrial wireless system under test where those emissions are not produced for communications purposes. Examples may include emissions from microwave ovens, welding stations, and variable speed drivers. In order to test an industrial wireless system prior to deployment, non-communications electromagnetic aggressors should be produced in a repeatable and controllable fashion. In this report, we introduce a playback approach for non-communications electromagnetic aggressor reproduction. The approach include signal measurements, data processing, and radio-based synthesis. Tungsten Inert Gas (TIG) welding emissions at the 2.4 GHz frequency band were reproduced to validate the approach using a software-defined radio for signal reproduction.

Keywords

welding; electromagnetic interference; industrial wireless; smart manufacturing; factory communications; RF; IEEE 3388.

Table of Contents

List of Tables

List of Figures

1. Introduction

An industrial wireless system (IWS) consists of a number of industrial wireless networks (IWNs) for data communications between operational industrial equipment. An IWN is a wireless network that is responsible for transferring signals between various industrial processes that carry related information to the underlying industrial process. The performance of a specific IWN is usually assessed under ideal conditions. However, ideal conditions rarely occur in these settings. Several factors (aggressors) exist that could degrade the performance of an industrial wireless system. Aggressors can be classified based on their nature into physical and electromagnetic. The surroundings of an industrial wireless system defines its physical aggressors. Electromagnetic aggressors are systems that produce electromagnetic emissions that impact the communications performance of the industrial wireless system under test. The emerging IEEE P3388 [1] standard provides a reference test architecture for the performance evaluation of industrial wireless systems and an assessment process for various industrial wireless use cases.

A classification of industrial wireless aggressors is shown in Fig. 1. Physical aggressors are defined by the impact of the surrounding environment on the transmissions of the IWN under test through specifying the wireless channel characteristics between the nodes of the IWN. Categories of electromagnetic aggressors include communications-based interference and non-communications-based interference. Coexisting communications-based interference may include other networks, adjacent channel activity, and a raised noise floor from poorly filtered adjacent channel transmissions. Non-communications-based interference may originate from machinery in the surrounding environment or intentional jamming.

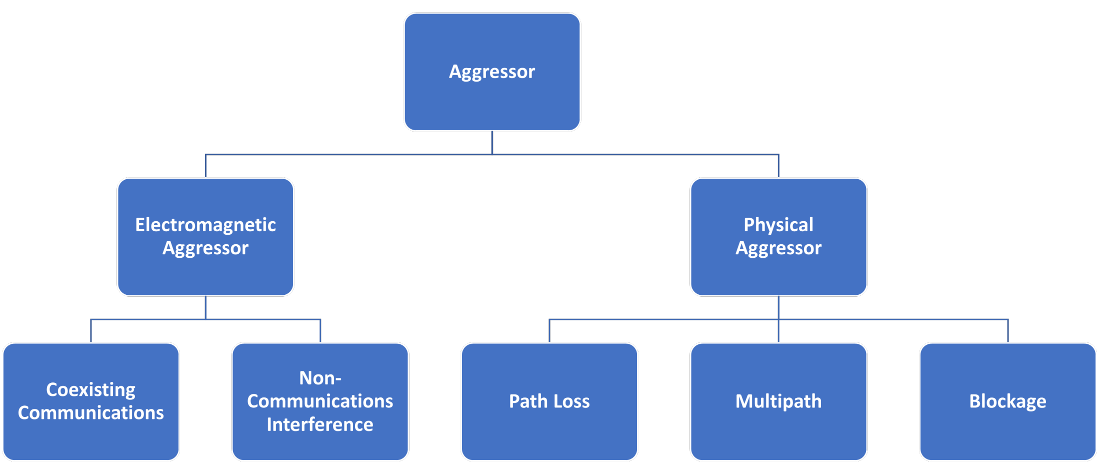

Fig. 1. Industrial Wireless Aggressor Classification based on their nature and source.

In industrial environments, in addition to interference resulting from various communications networks, equipment can also produce electromagnetic over-the-air (OTA) emissions that may occupy the radio spectrum. As an example, we measured the OTA activity from a Tungsten Inert Gas (TIG) welding station and found that it produces interference in the 2.4 GHz band [2]. In general, the source of electromagnetic emissions can be varying electric current in equipment, the high electric power values used, or the electromagnetic emissions that are produced in the industrial process itself. Some of these sources could have very wide-band emissions [3, 4]. However, the band of interest and the focus of this work is the band where the deployed industrial wireless network operates.

Adoption of wireless networks can be made more acceptable if the uncertainty of the wireless medium is better understood and wireless devices are designed to accommodate such uncertainty. This can be achieved through analysis of the RF environment beyond its propagation characteristics and the standardized evaluation of wireless network performance prior to deployment [5]. One of the most difficult steps in testing wireless networks for deployment is emulating and reproducing the interfering networks that may exist in the deployment environment. The ability to reproduce the electromagnetic aggressors in an experimental wireless platform provides repeatable and reproducible experimental testing and allows for the creation of large datasets under various circumstances [6, 7].

In this report, we discuss the various options for reproducing non-communications electromagnetic aggressors from the signal processing and wireless equipment viewpoints. We further discuss the required properties of the reproduced signals to fulfill the testing needs. Then, we introduce a playback approach for non-communications electromagnetic aggressor reproduction and describe its various processing steps such as signal measurements, data processing, and electromagnetic signal synthesis. Finally, we demonstrate the approach through a validation example for TIG welding emissions at the 2.4 GHz frequency band using a Universal Software Radio Peripheral (USRP) for signal reproduction.

2. Industrial Wireless non-Communications Aggressor Reproduction

2.1. Reproduction Process Entities

While reproducing non-communications electromagnetic aggressors, a number of related entities should be considered. The specific connections between entities will depend on the reproduction process. General definitions are discussed below:

- Non-communications measured data: The recorded data of the electromagnetic aggressor where the signal type, format, and resolution depend on the measurement equipment and process.
- Signal Processing: The set of data transformation techniques that are applied on the measured data to prepare it for reproduction.
- Reproduction Equipment: The equipment used to reproduce the aggressor over the air, which may perform further data processing steps as well.
- Reproduced Aggressor: The over-the-air signal that is produced by the reproduction equipment and should have similar impacts of the original aggressor on the IWN at the frequency band of interest.
- Testing Scenario / Testbed: The scenario or the testbed where the reproduced aggressor should be applied to study the impacts of the non-communications aggressor on that scenario.

2.2. Characteristics for Reproduced Aggressors

In order to achieve the goals from reproducing non-communications aggressors, a set of characteristics should be evaluated. The specific metrics corresponding to these characteristics differ depending on the specific aggressor and application scenario. The connections between various entities and the corresponding characteristics are shown in Fig. 2.

- Accuracy: The measure of how close the reproduced aggressor to the original non-communications aggressor. Various error or correlation metrics can be used to measure the accuracy of the reproduced aggressors.
- Controllability / Interactivity: is the measure of the ability to control the parameters of the reproduced aggressors and the reproduction equipment including its power level, frequency band, and temporal characteristics.
- Repeatability: The closeness of agreement between independent instants of the reproduced aggressor to be able to test other scenario parameters independently. This definition covers the signal processing and reproduction equipment entities and their repeatability characteristics.

- Computational Efficiency: The amount of time, memory, and/or processing power required for the applied signal processing techniques to transform the measured data into the required form for the reproduction equipment.
- Integrability: The ability of the reproduced aggressor to be interconnected to the application scenario or testing environment using over-the-air transmissions, coaxial cables, or any other mean of connectivity.

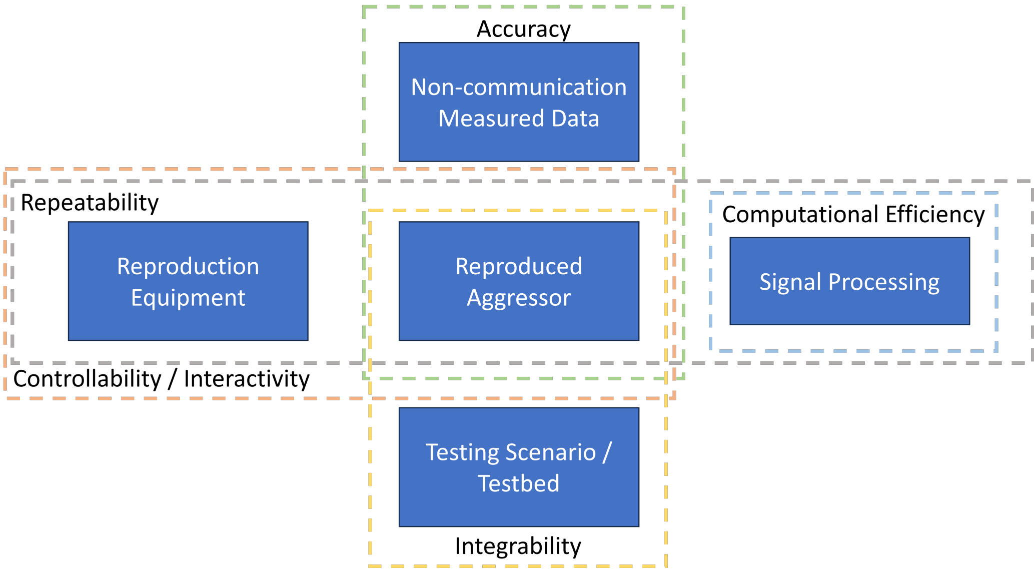

Fig. 2. Required characteristics for aggressor reproduction.

2.3. Approaches for Aggressor Reproduction

Reproduction of non-communication electromagnetic aggressor can follow a number of approaches in signal generation. These approaches are different from the viewpoint of signal processing and data generation. However, similar reproduction equipment can be used as discussed in [6–8]. Examples of widely used techniques are in the following.

- Playback of Measured Signal: An approach where the measured signal is recorded, processed to format for the reproduction equipment, and then played back in a controlled fashion.
- Statistical Modeling and Generation: An approach where the measured signal is statistically modeled, such as Markov modeling. The model is then used to generate signals that statistically follow the aggressor model.
- Generative Neural Networks: Another modeling approach that uses generative neural networks for modeling the aggressor behavior and generates signals that follow that behavior.

3. A Playback Approach for Aggressor Reproduction

In order to deploy a playback approach for reproducing electromagnetic measurements for experimental studies, high quality measurements have to be captured and processed for playback. Fig. 3 represents the proposed playback approach and various phases of the process. Each of the signal processing blocks will be used only when needed. The need for specific blocks depends on the measured data and the required characteristics for aggressor reproduction. Each block is defined as follows:

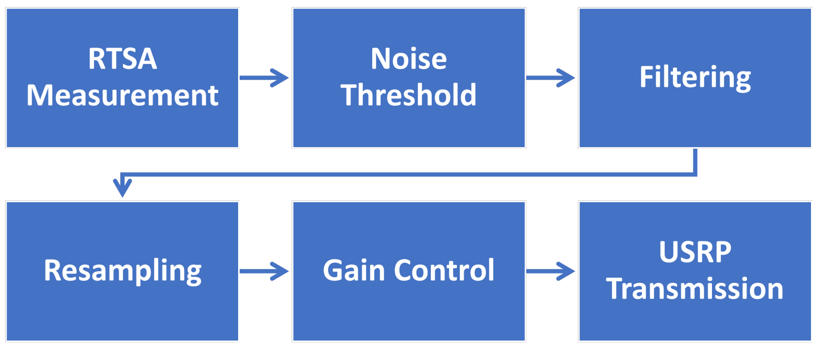

Fig. 3. Measured aggressor playback approach.

- Real time spectrum analyzer (RTSA) Measurement: A high-resolution measurement is captured in the IQ format for a period that is long enough to represent the measured aggressor. The sample rate is set at least four times the measurement bandwidth.
- Noise threshold: Any part of the recorded data that is below the noise floor does not represent the aggressor and must be removed before further processing of the signal.
- Filtering: Before downsampling the signal to be ready for the playback, a low-pass filter is used to prevent aliasing as a result of the downsampling process.
- Resampling: The reproduction equipment sample rate and bandwidth determine the playback sample rate that is achieved in this resampling step which also determines the bandwidth of the filter in the previous step.
- Gain control: A gain control function is used to maximize the digital power level of the interference signal going into the USRP transmitter while maintaining signal purity prior to transmission (e.g., avoiding digital and analog saturation).
- USRP Transmission: A USRP is used to stream the convert the digital interference signal to an over-the-air analog signal. Antenna gain and spatial pattern should be considered as a part of the reproduction process.

4. TIG Welding Aggressor Signal Measurement and Characteristics

As an example of non-communications interference, we consider TIG welding electromagnetic emissions. The welding machine used is the Miller Syncrowave 350LX, which is set up for applying AC current of 200 Amperes. It was used to weld an aluminum plate with supplied Argon gas. To capture the corresponding electromagnetic emissions, we used a Rhode and Schwartz spectrum analyzer with 160 MHz of instantaneous real-time bandwidth and a TSA900 directional ultra-wideband PCB Tapered Slot antenna with a frequency range from 900 MHz to 12 GHz. The antenna was placed 4 meters from the welding location. A photo of the welding location at the far side of the table and the measurement antenna is shown in Fig. 4.

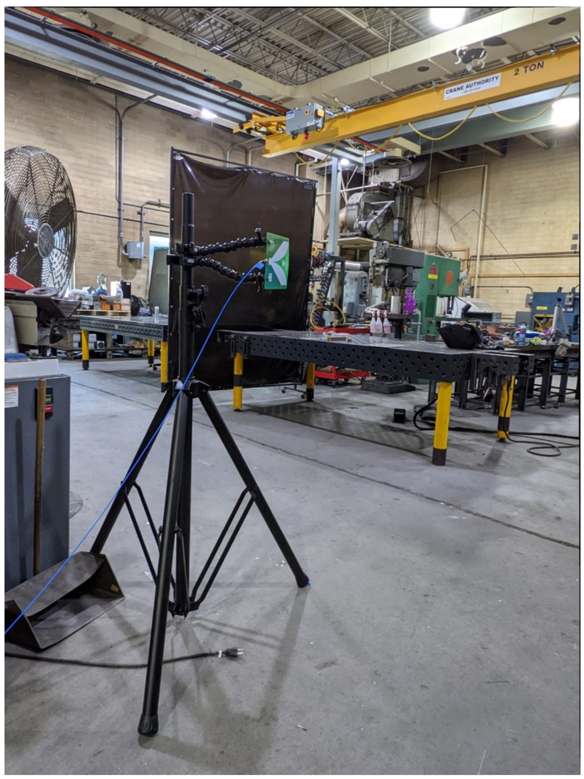

Fig. 4. The NIST machine shop welding station and measurement antenna.

We measured the spectrum of the measured TIG welding in the 900 MHz and 2.4 GHz bands. The spectrum on both bands was found to be almost flat over each of the bands. The time-domain signal was found to be formed as a pulse train where random idle periods existed, as shown in Fig. 5. The measurements were sampled at a rate of 625 Msamples/second. The measured signal follows an almost periodic on-off pattern while the pulses are not identical. The exact amplitudes of the pulses randomly vary and the intervals between the pulses are not exactly the same.

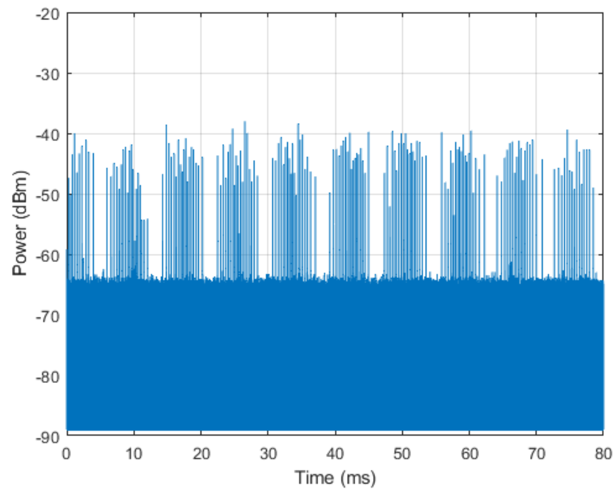

Fig. 5. The time-domain measured data at 2.4 GHz.

In Fig. 6, we zoom in to one of the pulses to further understand the structure of the measured welding signal. Multiple non-uniform impulses of different power levels composing each of the pulses from the TIG welding signal including smaller idle periods.

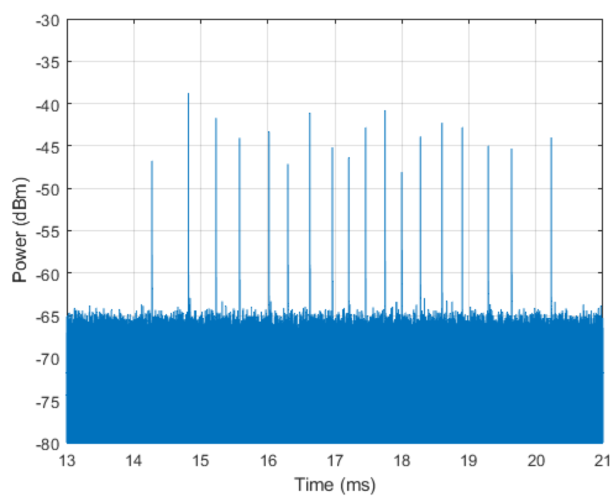

Fig. 6. The composition of one TIG welding pulse.

At a very small time scale, we look into the shape of the impulses composing the TIG welding signal. In Fig. 7, the shape of an impulse follows an exponential decay after a relatively very fast rising edge.

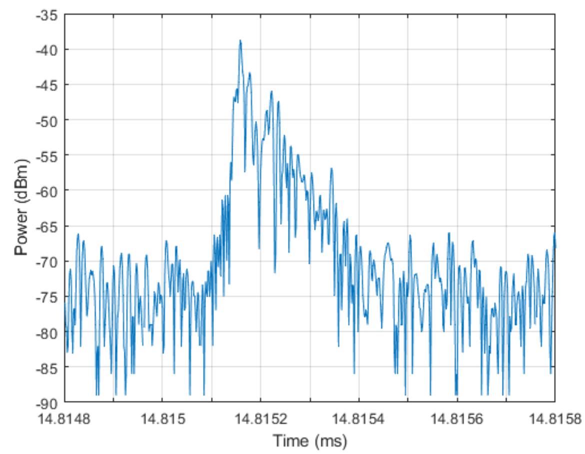

Fig. 7. A deeper look into the impulses of the TIG welding signal.

Additionally, we present the histogram of the impulse peak power levels of the measured TIG welding signal in Fig. 8. The peaks of the impulses vary approximately over a range of 12 dB and cannot be directly approximated using a fixed value.

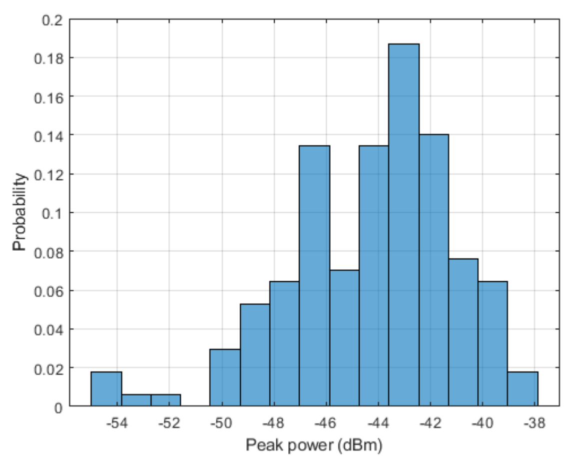

Fig. 8. The histogram of the impulse levels within the measured TIG welding signal.

As a result, the process of modeling the TIG welding signal is not straight-forward using traditional modeling techniques. The variation of the signal at time domain happens on multiple scales where the larger scale of tens of milliseconds can be almost characterized by a periodic signal. The second time scale is a random process that generates impulses with peak powers following the histogram. The third time scale is the shape of the impulses which follows an exponential pulse shape. Note that, depending on the network under test and its time scale, a modeling approach can be implemented. However, capturing all the characteristics of the measured welding signal in high-fidelity would be computationally expensive, as shown in [2].

Additionally, the signal at 900 MHz is also measured using the same exact settings for the welding apparatus and the measurement equipment. In Fig. 9, the time-domain signal at center frequency of 900 MHz follows similar pattern to the signal at 2.4 GHz band. The observed difference of the measured signal at 900 MHz was the power level. The difference in power is due to the difference in path loss and the difference in Fourier harmonic level at these frequencies of the arc weld driving pulse train.

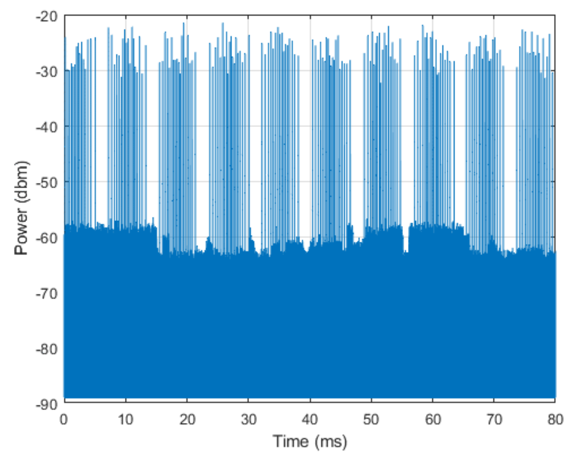

Fig. 9. The time-domain measured TIG welding signal at 900 MHz.

To further validate the similarity between measured signals at 900 MHz and 2.4 GHz, the curves of the cumulative density function (CDF) of the impulse peak levels within the measured TIG welding signals at the two center frequencies are presented in Fig. 10. The curves at both frequencies follow the same trend and have similar patterns but shifted in the impulse peak levels.

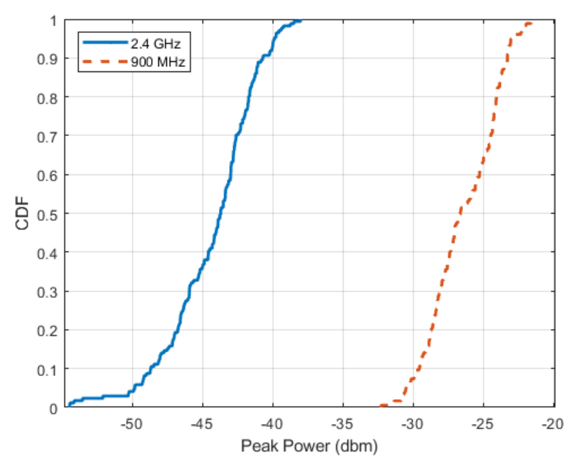

Fig. 10. The cumulative density function of the impulse peak levels within the measured TIG welding signal at 900 MHz and 2.4 GHz.

The propagation path loss is dependent on the signal frequency (or, inversely, the wavelength) of the interference signal [9]. In addition to the path loss dependency on frequency, we hypothesize that the source of these signals at 900 MHz and 2.4 GHz is a result of the high frequency harmonics emanating from the high-frequency (HF) modulation of the TIG arc generator or the arc itself. This high frequency modulating signal is a periodic pulse train at 27 MHz where the harmonic coefficients get smaller geometrically at higher frequencies in accordance with a Fourier Series expansion.

5. TIG Welding Aggressor Playback

In order to be able to integrate the TIG welding signal in various scenarios, we describe an approach for adapting the playback TIG welding signal against distance from the TIG welding apparatus and the center frequency of the wireless network under test. The focus in this section is to adapt the power level of the TIG welding signal. The adaptation allows to run the playback approach when the network under test is located at a different distance than the measured TIG welding distance and operates at a different frequency band.

5.1. Signal Fitting and Adaptation

We considered two sources for varying the power of the TIG welding signal, namely, the path loss and the level of the harmonics resulting from the TIG welding high frequency driving pulses. Let us denote the pulse rate of the driving pulses by R_{w}, which has a typical value of 27 MHz. The pulse shape of the driving pulse train was fitted using the measured data. In this work, we considered Trapezoidal pulses with rise time of zero and a variable fall time. The assumption of negligible rise time follows the measured pulse shape, as shown earlier. We denote the complex-valued Fourier coefficient value of the pulse train at a frequency f as $H(f)$. Additionally, we use the path loss equation for an indoor industrial environment in [10]. The path loss, denoted by PL_{LOS}, is defined as follows:

$$PL_{\mathsf{LOS}} = 31.84 + 21.5\ \log_{10}(d) + 19.0\ \log_{10}(f), \tag{1}$$

where d is the distance in meters and f is the frequency in GHz. The constants in the above equation are obtained using empirical data in multiple indoor industrial environments.

To tune the pulse shape to fit the obtained data at 900 MHz and 2.4 GHz that was measured 4 meters away from the welding apparatus, we denote the total TIG welding signal power in dB at a specific frequency and distance by $P_{\mathsf{w}}(f,d)$. For generalization of the tuning approach, we denote these two reference frequencies by f_1 and f_2, and the reference distance by d_{ref}. The fall time of the pulse is exhaustively searched to achieve the following condition

$$P_{\mathsf{w}}(f_1, d_{\mathsf{ref}}) - P_{\mathsf{w}}(f_1, d_{\mathsf{ref}}) = 20\log_{10}\frac{H(f_1)}{H(f_2)} + 19.0\ \log_{10}\frac{f_2}{f_1}. \tag{2}$$

Note that the pulse tuning condition depends only on the frequency difference as both signals are measured at the same reference distance.

Once the pulse shape is tuned to fit the measured data, the power of the playback signal at an arbitrary frequency band, f_x and distance d_x can be evaluated using the tuned pulse shape and the path loss equation as follows:

$$P_\mathrm{w}(f_x, d_x) = P_\mathrm{w}(f_1, d_\mathrm{ref}) - 20\log_{10}\frac{H(f_1)}{H(f_x)} - 19\log_{10}\frac{f_x}{f_1} - 21.5\log_{10}\frac{d_x}{d_\mathrm{ref}}. \tag{3}$$

5.2. Reproduction Example and Results

The process described in Section 3 is followed for the measured TIG welding signal to make it ready for reproduction. The playback approach was selected due to the complexity of the TIG weld signal. The selected reproduction equipment was the USRP X-300 that is a high-performance, scalable software-defined radio (SDR) platform. The daughterboard used was UBX-160 that has a full-duplex wide-band transceiver and covers frequencies from 10 MHz to 6 GHz and an instantaneous bandwidth at the transmitter of 160 MHz.

The data was processed using Matlab to get the IQ time-domain samples to be ready for streaming. To stream the processed data through the USRP, we used GNU Radio software toolkit. GNU Radio is a free and open-source software development framework that provides signal processing blocks to implement software radios and can be used with RF hardware to control the SDRs. The processed data was streamed to the USRP using a 10 Gbps network interface to avoid any underflows in the USRP buffers that can occur from starving the input queue. Gain control was performed using by selecting a maximum digital gain prior to streaming samples to the USRP. The gain control is applied to achieve the right power following the adaptation procedure to reproduce the TIG welding signal level in accordance with the distance and frequency requirements of the test scenario. In some case, the required power of the testing scenario cannot be achieved using the rated power output of the USRP; therefore, a power amplifier may be deployed in such cases.

We performed the various signal processing steps using Matlab where the recorded IQ data is initially imported. We applied a simple noise threshold to remove any samples below that threshold. The threshold was tuned to allow only for the samples that were considered part of the signal that should be reproduced. We used the Matlab decimation Chebyshev default filter for the downsampling. Some FIR filters can be more computationally efficient for larger sizes of data. The downsampling process may require interpolation if the new sampling rate is not an integer divisor of the original sampling rate.

The reproduction error is measured using the relative mean squared error (RMSE) which is defined as the ratio between the mean of the squared error between the reproduced signal and the original measured TIG welding signal to the mean of the squared original signal. The evaluation equation can be stated as

$$RMSE = \frac{E[(Reproduced - Original)^2]}{E[Original^2]}, \tag{4}$$

Table 1. Reproduction Parameters and Metrics

Parameters and Metrics	Values
Measurement Parameters	
Center Frequency	2.45 GHz
Resolution Bandwidth	160 MHz
Sample Rate, F_s	625×10^6 Hz
Capture Length	80 ms
Reproduction Process Parameters	
Playback Sample Rate, F_r	125×10^6 Hz
Filter Order	30
Noise Threshold	-64 dBm
Performance Metrics	
RMSE	0.305

where $E[\cdot]$ is the expectation. In order to calculate the error, we aligned the reproduced signal to the original signal using a correlation approach where we applied a simple linear interpolation to the reproduced signal and then aligned the interpolated signal to the original signal to get the maximum correlation between the two signals. A summary of the used parameters and results are shown in Table 1.

Additionally, in Fig. 11, we present the reproduced signal in comparison to the original signal at the level of the impulse shape. This figure demonstrates the closeness of the reproduced signal to the original signals. The main causes for the differences between them are the downsampling and filtering of the original signal before playback.

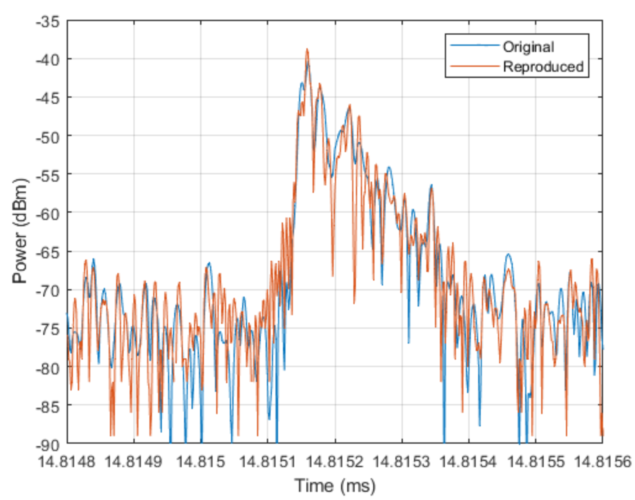

Fig. 11. Comparison between the reproduced signal and the original signal.

The histogram of the impulse peak power levels of the reproduced signal is shown in Fig. 12. This figure can be compared to the histogram of the original signal in Fig. 8. Both histogram show similar trends and very close values.

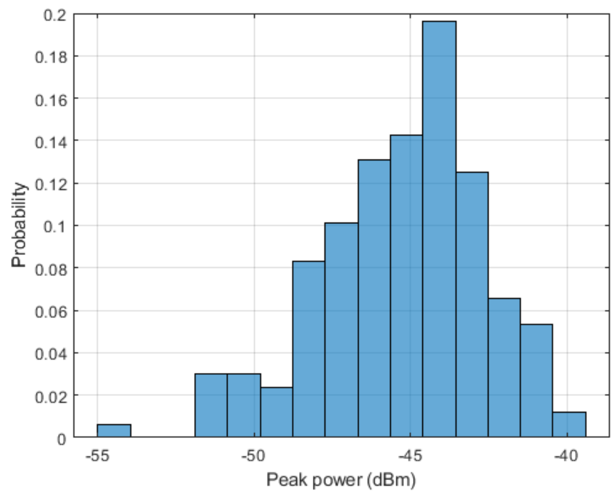

Fig. 12. The histogram of the impulse levels within the reproduced TIG welding signal.

6. Conclusions

In this report, we described and demonstrated the use of a playback approach for a TIG welding data signal reproduction. This approach can be further generalized for various non-communications electromagnetic signal aggressors. The use of playback approach in non-communication aggressor reproduction is favorable compared to other modeling approaches because of the higher computational efficiency and ease of implementation. However, applying this approach for non-communication interference presents a challenge in that the interference signal must be captured in advance. It is even more challenging when the characteristics of the interference could change significantly from site to site.

Future directions include the tuning of reproduction process parameters to optimize the performance. These parameters include signal processing and over-the-air signal generation parameters. More performance evaluation metrics need to be defined and assessed to capture the various characterizing requirements of the reproduced signal compared to the original measured signal. Additionally, the output power of the used USRP is limited, and hence, a power amplifier could be used to achieve the required power level of the over-the-air aggressor signal in some cases.

The widespread adoption of interference reproduction for testing and performance assessment of industrial wireless systems requires large amounts of measurement data for various non-communications aggressors. The characteristics of a measured signal can be dependent on the model of interference-generating equipment, the operational environment, and process parameters. In a welding scenario, the interference signal depends on the welding technology, the welded material, the welder model, the electrode material, and the used gas type. As a result, measuring the resulting interference signals at various welidng scenarios can be beneficial to define the common characteristics of welding signals and the other features that will be scenario-dependent. Creating a database for non-communications electromagnetic interference would be beneficial for improved testing of industrial wireless systems.

In this report, we have introduced an power adaptation technique for the interference signal to be able to reproduce the welding signal at different frequency band and distance than the ones at which the welding interference is measured. The introduced technique is suitable for TIG welding signals because of the high frequency driving pulses. The need for adapting the measured signal for playback is essential to allow for the generalization of the playback approach. In general, extrapolation and interpolation techniques can be used for adapting the measured signal features. However, the accuracy of the resulting playback signal will depend on the used interpolation and extrapolation schemes and the closeness of resulting signal coordinates to the measured signal.

References

[1] Candell R IEEE P3388 working group - P3388 wireless performance assessment and measurement working group. Available at https://sagroups.ieee.org/p3388/.

[2] Hany M, Geng J, Montgomery K, Candell R (2024) On the Impact of TIG Welding Interference on Industrial Wi-Fi Networks: Modeling of Empirical Data and Analytical Studying of Coexistence (The 7th IEEE International Conference on Industrial Cyber-Physical Systems (ICPS), St. Louis, MO, US). Available at https://tsapps.nist.gov/publication/get_pdf.cfm?pub_id=956781.

[3] Schaffenroth S, Schmidt HP, Kölpin A (2022) Measurement setup for industrial communication techniques under electromagnetic interference. *2022 IEEE Sensors Applications Symposium (SAS)*, pp 1–6. https://doi.org/10.1109/SAS54819.2022.9881364

[4] Candell R, Kashef Hany M, Perez-Ramirez J, Conchas J (2023) An ieee standard for industrial wireless performance evaluation. *IEEE Internet of Things Magazine* 6(1):82–88. https://doi.org/10.1109/IOTM.001.2200069

[5] Villa D, Tehrani-Moayyed M, Robinson CP, Bonati L, Johari P, Polese M, Melodia T (2024) Colosseum as a digital twin: Bridging real-world experimentation and wireless network emulation. *IEEE Transactions on Mobile Computing* :1–17https://doi.org/10.1109/TMC.2024.3359596

[6] Hithnawi A, Kulkarni V, Li S, Shafagh H (2015) Controlled interference generation for wireless coexistence research. *Proceedings of the 2015 Workshop on Software Radio Implementation Forum* SRIF '15 (Association for Computing Machinery, New York, NY, USA), p 19–24. https://doi.org/10.1145/2801676.2801682. Available at https://doi.org/10.1145/2801676.2801682

[7] Burns TL, Martin RP, Ortiz J, Seskar I, Stojadinovic D, Davis R, Camelo M (2021) Synthetic wireless signal generation for neural network algorithms. *2021 IEEE Conference on Standards for Communications and Networking (CSCN)*, pp 174–179. https://doi.org/10.1109/CSCN53733.2021.9686084

[8] Politis C, Maleki S, Duncan JM, Krivochiza J, Chatzinotas S, Ottesten B (2018) SDR Implementation of a Testbed for Real-Time Interference Detection With Signal Cancellation. *IEEE Access* 6:20807–20821. https://doi.org/10.1109/ACCESS.2018.2825885

[9] Candell R, Hany M, Lee KB, Liu Y, Quimby J, Remley K (2018) Guide to industrial wireless systems deployments (National Institute of Standards and Technology, Gaithersburg, MD), https://doi.org/10.6028/NIST.AMS.300-4. Available at http://nvlpubs.nist.gov/nistpubs/ams/NIST.AMS.300-4.pdf

[10] (2020) 5G; Study on channel model for frequencies from 0.5 to 100 GHz ((3GPP TR 38.901 version 16.1.0 Release 16)),